Talanta 160 (2016) 256–267

Contents lists available at ScienceDirect

Talanta

journal homepage: www.elsevier.com/locate/talanta

The development of a quantitative and qualitative method based on UHPLC-QTOF MS/MS for evaluation paclitaxel–tetrandrine interaction and its application to a pharmacokinetic study

Dan Li [a,b], Zhonglian Cao [a], Xueling Liao [a], Ping Yang [a,*], Li Liu [b,*]

[a] School of Pharmacy, Fudan University, Pudong, Shanghai, 201203, PR China
[b] Center for Pharmacological Evaluation and Research of SIPI, Shanghai Institute of Pharmaceutical Industry, Shanghai, 200437, PR China

ARTICLE INFO

Article history:
Received 1 May 2016
Received in revised form
2 July 2016
Accepted 8 July 2016
Available online 8 July 2016

Keywords:
UHPLC-QTOF MS/MS
Paclitaxel
Tetrandrine
Surface plasmon resonance (SPR)
Drug–drug interaction (DDI)

ABSTRACT

Paclitaxel is a broad-spectrum anti-cancer drug by targeting microtubulin. However, multidrug resistant (MDR) makes its clinical application more difficult and results in failure of chemotherapy. Tetrandrine as a potential multidrug resistant modulator could be combined with other anti-cancer drugs. In this study, ultra-performance liquid chromatography (UHPLC) combined with quadrupole time-of-flight mass spectrometry (QTOF) was applied to simultaneously qualitative and quantitative analysis of paclitaxel for the pharmacokinetic studies while combined with tetrandrine. This method was developed based on non-target screening mode IDA (Information Dependent Acquisition). As a result, the validated range was 0.25–64 ng/ml (30 μl plasma) for paclitaxel. Totally 33 metabolites of paclitaxel and tetrandrine were identified in vivo and in vitro. The main metabolites of PTX were dose-dependent decreased with different amounts of tetrandrine co-administration no matter in vivo and in vitro, the exposure of PTX increased in pharmacokinetic study. The verified method is sensitive accurate and effective for the simultaneous determination of paclitaxel and its metabolites in blood, urine and live microsome incubation samples and it was successfully applied to evaluate the pharmacokinetics and drug–drug interaction between paclitaxel and tetrandine. Furthermore, a biosensor technology, surface plasmon resonance (SPR) analysis was applied to preliminary evaluate the competitive protein binding of multiple components. The SPR analysis indicated that the affinity between 6-hydroxy-paclitaxel and micotubulin is similar to that between paclitaxel and micotubulin, and tetrandrine also does not form a competitive combination with paclitaxel. For human, 6-hydroxy-paclitaxel is the one of main metabolites of paclitaxel, so the results suggested that tetrandine has an influence on the metabolite of paclitaxel, but tetrandine and the main metabolites of PTX probably do not affect PTX's biological targeting, the effect of its pharmacological action needs to be further studied.

1. Introduction

Paclitaxel (PTX) is a broad-spectrum anti-cancer drug that isolated from the bark of pacific yew tree, Taxus brevifolia, PTX could promote and stabilize the polymerization of microtubulin and further prevent the physiological process of mitosis in cell [1,2]. It is used for patients with breast cancer, ovarian cancer, esophageal carcinoma or non-small-cell lung cancer [3–6]. However, the phenomenon of multi-drug resistance(MDR) is common in clinical cancer treatment [6,7] and tumor cells could induce MDR by enhancing the P-glycoprotein (*p*-gp) expression or other pathways [8,9]. In addition, the PTX possesses the poor aqueous solubility and low oral bioavailability [10,11]. All of these factors make this chemotherapy more difficult or failure. To cope with this challenge, several strategies are being developed, such as multiple drug combination to overcome MDR and eliminate undesired side effects [12–15], development new preparation to improve the solubility and so on [16,17]. In clinical treatment, the multiple drug combination is very common for improving the efficacy and reversing the drug resistant [18].

Tetrandrine (TTD) is an effective botanical drug with strong ability of reversing the multidrug resistance of tumor cells by inhibiting the drug efflux activity of P-gp [19–22], so that in clinical application it could be combined with other drugs to treatment patients [23]. Previous researches have indicated that TTD could induce cell cycle arrest and apoptosis in several different cancer cell lines [24–28], and synergistic effect on the cytotoxicity of

* Corresponding authors.
E-mail addresses: yangping@fudan.edu.cn (P. Yang), liulisipi@foxmail.com (L. Liu).

http://dx.doi.org/10.1016/j.talanta.2016.07.022
0039-9140/

chemotherapeutic agents had been found [27]. P-Glycoprotein-mediated multidrug resistance to PTX could be reversed through co-delivery TTD and exhibited significantly improved antitumor efficacy [22,29]. These researches effort focus on exploring the synergistic anticancer effects between TTD and PTX. Some papers have reported the pharmacokinetic studies about PTX combined with drugs like trebananib [30], dexamethasone [31], Chinese herbal formula [32] and NVP-BHG712, the inhibition of the ABCC10 transporter [33]. These data suggest that the monitoring of the pharmacokinetics of paclitaxel is recommended. But limited studies exist on the pharmacokinetic study and metabolite variation of PTX in combination with tetradrine, and further studies will be needed to evaluate the competitive protein binding of PTX, PTX's metabolites and tetradrine. In China, TTD as a herbal medicine is used to treat hypertension, inflammation, liver fibrosis and other diseases [34–36]. However, TTD could affect the activity of CYP3A4 which is one of the important metabolic enzymes [37]. Most of drugs (including paclitaxel) were proved that they metabolized to their metabolites by various metabolic enzymes especially CYP3A4 [38]. Thus, the metabolite of PTX could be affected by TTD in vivo and in vitro. Hence, it is necessary to clarify how TTD affect the metabolism of PTX and the quantitation of this drug together with its main metabolites is also of great essential.

Here, the quantitative and qualitative method based on information-dependent acquisition (IDA) acquisition of ultrahigh-performance liquid chromatography-quadrupole time-of-flight mass spectrometry (UHPLC-QTOF MS/MS) would be used for evaluation the effect on pharmacokinetic behavior of PTX combined with TTD in vivo and in vitro. Many different analytical methods have been used for quantitative analysis of paclitaxel such as tubulin-based quantitative assay [39], Protein-Based Bioassay [40], HPLC with UV detector [41], fluorescence polarization immunoassay (FPIA) [42], cathodic stripping square wave voltammetry [43], Fluorescence Immunoassay [44], liquid chromatography–mass spectrometry(LC–MS) [45], liquid chromatography-ion trap mass spectrometry method [46], LC–MS–MS [47,48], liquid chromatography-tandem triple-quadrupole mass spectrometry [49]. LC–MS–MS could be used to determine the PTX and its main metabolites [48,50], but there is no method which could meet qualitative and quantitative analysis for PTX and its possible metabolites in biological samples meanwhile. In our study, the method based on IDA acquisition of UHPLC-QTOF MS/MS allowed simultaneous quantification and identification of PTX and its metabolites with sample prepared by protein precipitation [51] and liquid–liquid extraction (LLE) [48,52]. The method can be regard as a suitable tool to evaluate the pharmacokinetics and interaction between PTX and TTD. Furthermore, it will help to explore the interaction between PTX and other drugs.

Surface plasmon resonance (SPR) is regularly exploited in the kinetic analysis of biomolecular interactions and small-molecule drug-discovery, hit-validation studies. It has become a standard tool in biopharmaceutical research and development [53,54]. The ability to determine association and dissociation kinetics for molecular interactions provides detailed insights into the mechanism of complex formation. In our research, this technology is useful to make a prediction about the efficacy distinction between paclitaxel and its main metabolite and to preliminary assess the competitive binding of combination drugs with target protein. Furthermore, the results will assist in adjusting drug combination strategy.

2. Experimental

2.1. Materials

PTX (purity $>98\%$) was purchased from the National Institute for the Control of Pharmaceutical and Biological Products (Beijing, China). HPLC-grade acetonitrile (ACN) and methanol were purchased from Merck (Darmstadt, Germany), ethanol was purchased from sinopharm chemical regeat co.ltd. Ultrapure water was purified using a Milli-Q water purification system (Millipore, Bedford, MA, USA). Kinetex Phenyl-Hexylcolumn (1.7 μm, 2.1 mm × 100 mm) (phenomenex. USA). 6-hydroxy-paclitaxel (6-OHPTX) was purchased from J&K®. Tetrandrine was a gift of Dr Jiekai Cheng. Docetaxel, fangchinoline and cremophor EL were purchased from aladdin®. All other reagents and chemicals were of analytical grade. Male Sprague-Dawley rat liver microsomes (Research Institute for Liver Diseases (Shanghai) Co. Ltd). The purified tubulin (Cytoskeleton, Denver), Dimethyl sulfoxide (Sigma, St. Louis, MO, USA), Standard Biacore materials and reagents were used, including: certified Biacore® HBS-EP running buffer (10 mM MHEPES pH value 7.4, 150 mM NaCl, 3 mM EDTA and 0.005% polyoxyethylenesorbitan surfactant), CM5 sensor chip, an amine coupling kit. All buffers were prepared using ultrapure water (Milli-Q, Millipore, Milford, MA).

2.2. Chromatographic conditions

Chromatography was performed on an UHPLC system (Angilent Corp., Milford, MA, USA) with a conditioned autosampler at 4 °C. The separation was carried out on an Kinetex Phenyl-Hexylcolumn (1.7 μm, 2.1 mm × 100 mm). The column temperature was maintained at 30 °C. The analysis was performed with gradient elution using (A) acetonitrile and (B) water containing 10 mmol ammonium acetate as the mobile phase. The gradient program as follow: linear gradient from 70%A to 60% in 5 min; then decreased to 40% A in the 4.4 min; 0.6 min followed by a gradient to10%A, held on 3 min 10%A changed to 70%A immediately then held at 70% A for 2 min for equilibrating the column. The flow rate was set 0.3 ml/min.

2.3. Mass spectrometric conditions

High mass resolution experiments were performed on a TripleTOF5600+ mass spectrometer (ABSCIEX) equipped with an ESI source in positive ion mode. The capillary and cone voltages were 2000 and 40 V, respectively. The ion source gas 1(GS1) and GS2 was set to 50 and 60, and the source temperature was 550 °C. An IDA experiment with a dynamic range enhancement (DRE) in full scan functions was applied. The mass data was acquired from 800 to 1000 Da for quantification and calibrated during acquisition using an external reference of sodium formate solution. The molecular weight was set from 500 to 1500 Da for identification the metabolites. The CE was set to 45 eV and the DP was set 80 eV, the mass range from 50 to 1200 Da for the acquisition of MS/MS data. The raw data was acquired and processed by using the analyst®TF1.6 software program. MultiQuant 2.1 was used to process the date for a quantitative analysis. What's more, PeakView 2.0 with chemspider database and MetabolitePilot 1.5 were used to process the spectrum for an identification study. In the IDA experiment, the full scan model was set to acquire all information of TOF MS and dynamic background subtract was applied to get the high quality data of product ions. Maximum four candidate ions were monitored per cycle.

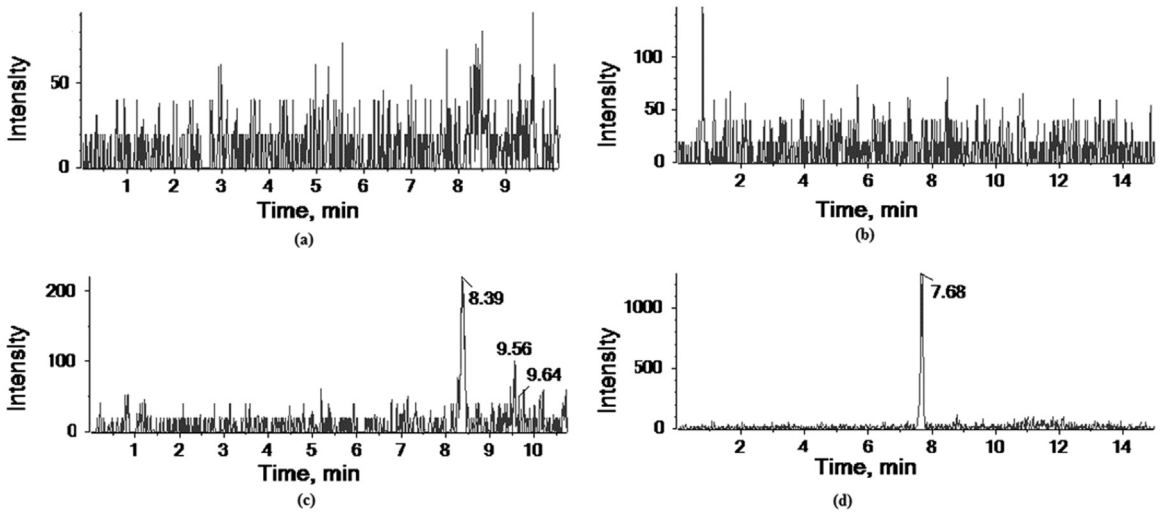

Fig. 1. The extrated ion chromatogram of PTX (a) and docetaxel (b) in blank rat plasma; The extrated ion chromatogram of blank plasma sample spiked with PTX at LLOQ of 0.25 ng/ml (c) and blank plasma sample spiked with docetaxel (10 ng/ml) (d).

Table 1
Extract recovery and matrix effects (n=5).

Analyte	Concentration	Extract recovery (%)	Matrix effects (%)
PTX	0.5 ng/ml	81.31 ± 6.84	109.83 ± 15.13
	4 ng/ml	96.39 ± 7.42	111.75 ± 13.75
	50 ng/ml	93.18 ± 3.14	104.71 ± 1.35

PTX: paclitaxel.

2.4. Method validation

2.4.1. Selectivity and sensitivity

The selectivity of the method was evaluated by comparing the blank plasma samples and the plasma samples containing analytes. There should be no potential interferences at the peak regions for analytes. Chromatographic peaks of PTX and internal standard (docetaxel 10 ng/ml) should be identified on the basis of their retention times. A sensitive quantitative method could measure plasma samples that contained the lowest concentration analyte. It requests the single noise ratio (SNR) should be larger than 10 at the lower limit of quantification (LLOQ) level concentration with acceptable precision and accuracy.

2.4.2. Linearity, precision and accuracy

The linearity of this quantitative method for the determination of PTX was evaluated by calibration curves in the range of 0.25–64 ng/ml (0.25, 0.5, 1, 2, 8, 16, 32 and 64 ng/ml). The calibration curves were obtained by plotting the ratios of chromatographic peaks response (paclitaxel/docetaxel). Least squares linear regression analysis was used to determine the slope, intercept and correlation coefficient (R^2). The calibration curve requires R^2 is 0.99 or better. To evaluate the precision, six quality control (QC) samples of three different concentrations (0.5, 4,50 ng/ml) were processed and injected at a single day (intra-day)and at different days (inter-day). The variability of determination was expressed as the relative standard deviation (RSD%) and the accuracy was described as the relative error (RE %) which was calculated as (observed concentration − theoretical concentration)/theoretical concentration × 100%. The criteria for acceptability of the data included accuracy within ± 15% relative error from the nominal values and a precision of within ± 15% relative standard deviation, except for lower limit of quantification (LLOQ), where it should not exceed ± 20% of accuracy as well as precision.

2.4.3. Recovery and matrix effect

The extraction recoveries of PTX from rat plasma was determined by comparing responses from regularly pre-treated QC samples with responses from the direct injection of pure analyte standard solutions at three QC concentration levels. The recovery of the PTX in rat plasma was examined five times. The matrix effect was defined as the ion suppression, enhancement on the ionization of analytes, which was evaluated by comparing the responses of the deproteinized samples of blank plasma spiked QC samples with those of the standard samples at equivalent concentrations. The matrix effect of internal standard is also evaluated.

2.4.4. Stability studies

The stability was tested including the processed sample stability, three freeze–thaws stability, short-term stability and long-term stability of PTX in low-, mid- and high-quality control samples. Freeze–thaw stability of the analytes was determined over

Table 2
Accuracy and precision.

Analyte	Spiked Concentration	Intra-day (n=6)			Inter-day (n=18)		
		Found (ng/ml)	Precision RSD (%)	Accuracy RE (%)	Found (ng/ml)	Precision RSD (%)	Accuracy RE (%)
PTX	LLOQ (0.25 ng/ml)	0.25 ± 0.01	4.03	−1.04	0.25 ± 0.01	4.38	0.39
	0.5 ng/ml	0.52 ± 0.03	5.78	4.00	0.53 ± 0.05	9.44	6.00
	4 ng/ml	3.84 ± 0.29	7.55	−4.00	4.19 ± 0.33	7.88	4.75
	50 ng/ml	51.36 ± 2.25	4.38	2.72	53.24 ± 4.24	6.70	6.48

PTX: paclitaxel. LLOQ: lower limit of quantification. RSD: relative standard deviation. RE: relative error. Calculated as (observed concentration − theoretical concentration)/theoretical concentration × 100%.

Table 3
Stability of sample.

Stability	Remaining (%) (n=5)		
	0.5 ng/ml	4 ng/ml	50 ng/ml
Long-term stability	102.4 ± 10.8	96.1 ± 9.3	102.1 ± 1.2
Short-term stability	100.9 ± 5.3	105.2 ± 9.5	104.3 ± 5.4
Freeze–thaw stability	102.0 ± 1.1	96.0 ± 5.8	106.5 ± 1.2
Processed sample stability	101.8 ± 2.1	98.0 ± 5.7	101.8 ± 4.3

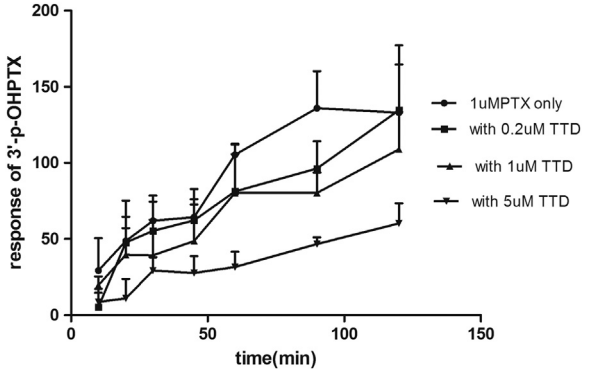

Fig. 2. The response-time curve of 3′p-OHPTX when PTX incubate with different concentrations of TTD (n=3).

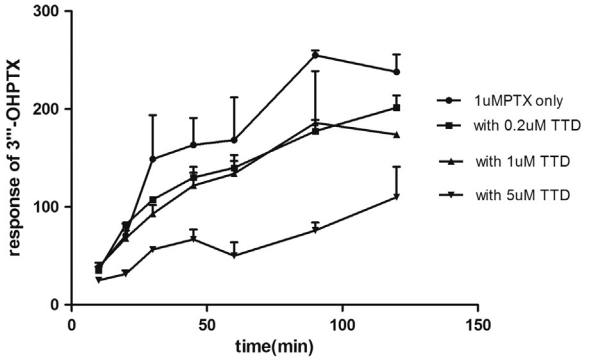

Fig. 3. The response-time curve of 3′-OHPTX when PTX incubate with different concentrations of TTD (n=3).

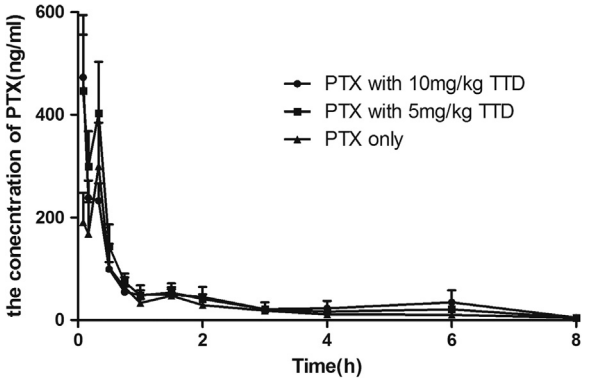

Fig. 4. The concentration-time curve of PTX with different concentrations of TTD (n=5).

three cycles. In each freeze–thaw cycle, the samples were frozen and stored at −20 °C for 24 h, then thawed at ambient temperature. To evaluate long-term stability, the samples were stored at −20 °C for two months. For the short-term stability, samples were kept at room temperature for 24 h before analysis. Due to every batch of samples were determined at 4 °C within 24 h. The processed sample stability was tested at 4 °C for 24 h.

Table 4
The parameters of drug-time curves of PTX (n=5).

Parameters	With 10 mg/ml TTD	With 5 mg/ml TTD	5 mg/ml PTX only
$t_{1/2}\alpha$ (h)	0.141 ± 0.085	0.107 ± 0.043	0.075 ± 0.033
$t_{1/2}\beta$ (h)	3.129 ± 0.904	2.861 ± 0.458	2.251 ± 0.489
$AUC_{0\sim t}$ (ng h/ml)	799.064 ± 199.207	981.264 ± 448.359	596.006 ± 290.785
$AUC_{0\sim\infty}$ (ng h/ml)	1039.894 ± 269.678	1194.085 ± 516.979	761.067 ± 348.552

PTX: paclitaxel. TTD: tetrandrine. $t_{1/2}\alpha$: distribution half-life. $t_{1/2}\beta$: elimination half-life. AUC: area under the curve.

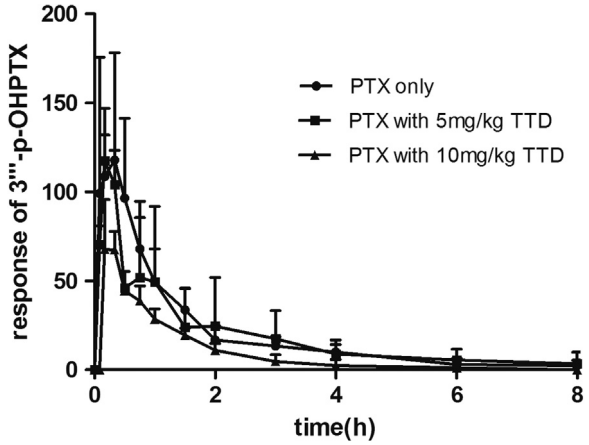

Fig. 5. The response-time curve of 3′-OHPTX when PTX combined with different concentrations of TTD (n=5).

2.5. Experiments and samples preparation

2.5.1. The metabolism of PTX and interaction with TTD in vitro

Applying the general procedure to incubate paclitaxel with liver microsomes, we set four groups. Control group is that the only paclitaxel (1 μM) in the Tris-HCl buffer (50 mM) containing $MgCl_2$ (10 μM) pre-incubate with Sprague-Dawley liver microsome (0.5 mg/ml) for 5 min, then NADPH (2 mg/ml)was added for initiation the reaction, finally the volume of incubation system was 200 μl which was incubated in the water baths shaker at 37 ± 1 °C and the whole systems were incubated for 10, 20, 30, 45, 60, 90, 120 min respectively; In other three groups, all compositions were same except different concentration TTD (0.2, 1, 5 μM) added respectively. This experiment repeated three times. In the end, 2 ml ice-cold acetonitrile was added for ending the reaction.

The microsome in incubation system was precipitated by acetonitrile first and then transfer 200 μl of the supernatant to the container (For identification, 1.5 ml supernatant should be transferred to container). The supernatant extracted by 2 ml methyl tert-butyl ether (MTBE). After centrifuged under 4000 g for 5 min, 1.5 ml supernatant should be dried under nitrogen at 40 °C. Then it was redissolved by 200 μl liquid of moving phase and 10 μl was injected into UHPLC system for analysis.

2.5.2. Pharmacokinetic study and sample preparation in vivo

The total fifteen Sprague-Dawley male rats (200 ± 20 g) (Shanghai Sippr-BK laboratory animal Co. Ltd.) were fasted for 12 h but free access to water and were randomly divided into three groups averagely (n=5): 1) In control group, rats were injected PTX alone through caudal vein at a dose of 5 mg/kg. 2) In drug-combination group, PTX (5 mg/kg) mixed with same dose of TTD

Table 5
The affinity between different compounds with microtubulin.

Compound	Ka	kd	KD	Concentration gradient (μM)					
PTX	1.51E+05	0.2573	1.71E-06	0.36	0.73	1.46	2.92	5.85	
6-OHPTX	1.39E+05	0.1458	1.05E-06	0.36	0.72	1.44	2.88	5.75	
PTX and 6-OHPTX	2.28E+05	0.4126	1.81E-06	0.36	0.73	1.46	2.92	5.85	For PTX
				0.18	0.36	0.72	1.44	2.88	For 6-OHPTX
TTD and PTX	2.91E+05	0.3586	1.23E-06	0.18	0.36	0.73	1.46		For PTX
				0.18	0.36	0.73	1.46		For TTD
TTD	1.33E+04	1.388	1.05E-04	1.25	2.5	10	20	80	

PTX: paclitaxel. TTD: tetrandrine. 6-OHPTX: 6-hydroxy-paclitaxel. Ka: association constant. Kd: dissociation constant. KD: affinity constant.

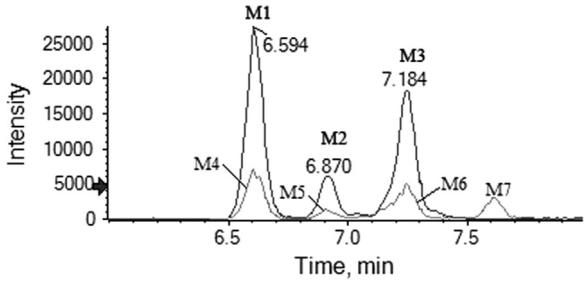

Fig. 6. The spectrum for metabolites of PTX.

were injected to rats body. 3) In another drug-combination, rats were injected PTX (5 mg/kg) mixed with double dose of TTD. Before injecting the drug, blank blood samples were collected via the ophthalmic veins of the rats by sterile capillary tube and blank urine samples were also collected. Whole blood samples were collected in heparinized polythene tubes respectively at 0.083, 0.17, 0.33, 0.5, 0.75, 1, 1.5, 2, 3, 4, 6, 8 h after drug injection. And immediately centrifuged it at 5000 rpm for 5 min to obtain plasma, and the tubes with plasma were stored at −20 °C for analysis. In this process, about 2 ml urine sample should be collected and immediately stored at −20 °C for analysis. In this part, TTD was dissolved in hydrochloric acid and diluted it to pH value 6.0 with PBS buffer. PTX was dissolved in ethanol with same volume cremophor EL and dilute it with six-fold PBS buffer.

The plasma samples were prepared as follows: 30 μl docetaxel (internal standard) methanol solution was added to 30 μl plasma sample, then 100 μl acetonitrile for precipitating proteins. And 100 μl water was added. After vortex-mixing for 30 s, 3 ml methyl tert-butyl ether (MTBE) was added to samples. After vortex-mixing for 15 min, samples were centrifuged at 4000 rpm for 10 min, and the 2 ml supernatant was transferred to another tube and evaporated to dryness at 40 °C under a gentle stream of nitrogen. The residue was reconstituted in 300 μl acetonitrile followed by vortex-mixing for 5 min. A 10 μl aliquot of the solution was injected to the UHPLC-QTOF MS/MS system for analysis. 1.5 ml urine samples were treated similarly but precipitate proteins for identification.

2.6. Tubulin binding and determination of affinity (Surface Plasmon Resonance (SPR) Assay)

The binding affinities of metabolites of Paclitaxel to α- and β-tubulins (recombinant 55 kDa monomers) were determined by the label-free, real-time Biacore T200 instrument (GE Healthcare, USA). Paclitaxel were used as positive control. Experiments were performed on research-grade CM5 sensor chip at 25 °C. The tubulin was immobilized to chip surface via amine coupling. The control flow cell was unimmobilized. The analyte was flow through the surface, the flow rate was 30 μl/min, the interaction was monitored in real time by the sensorgram. The specific binding were obtained after subtracting the response signal from the control flow cell. The kinetic analysis were evaluated with Biacore evaluation Version 3.0 software (GE Healthcare, Wisconsin, USA).

3. Results and discussion

3.1. Method development

3.1.1. Chromatography

In an appropriate chromatographic condition, mobile phase and elution program must be take into account as two of the most essential components. A proper chromatographic condition could separate the analytes completely as much as possible, increase the degree of analyte ionization, enhance the signal of analyte intensity in a reasonable analysis time. The acetonitrile–water systems was chose as the preferred phase for higher response and lower background noise provided than methanol. In addition 10 mmol ammonium acetate modifier in mobile phase was able to improve the peak shape and the ionization efficiency. The mobile phase and elution program was used as described in Section 2.2. The retention time was 8.37 min for PTX (876.3213), 7.18 min for 3′-OHPTX (892.3162) which is the main metabolite of PTX in rats, 7.68 min for docetaxel (830.3390). 3′-p-OHPTX (6.58 min) is another main metabolite of PTX in vitro, but in vivo the response of 3′-p-OHPTX is so lower than 3′-OHPTX that it cannot be determined continuously.

3.2. Method validation

3.2.1. Selectivity, sensitivity and matrix effect

The signal noise ratio (SNR) was more than ten times at the concentration of 0.25 ng/ml (SNR=10.70). Therefore it was choose as the LLOQ with good precision and accuracy (Table 2). The extracted ion chromatogram (EIC) of PTX and docetaxel in blank plasma and the EIC of blank plasma sample spiked with PTX at LLOQ of 0.25 ng/ml and blank plasma sample spiked with internal standard docetaxel (10 ng/ml) are represented in Fig. 1. And there is no obvious endogenous peaks to interfere PTX (8.37 min), 3′-OHPTX(7.18 min) and docetaxel (7.68 min). Therefore, it was selective enough to quantify PTX. Matrix effects must be tested in the analysis of mass spectrometry. The matrix effects of PTX for three QC levels were 109.83%, 111.75%, and 104.71%, respectively (Table 1). The matrix effect was 99.78 ± 2.99% for docetaxel. Overall, in this study, there is no significant matrix effects (e.g., ion suppression or enhancement) to interfere analysis since a little enhanced matrix effect was consistent and negligible in the present MS conditions.

3.2.2. Linearity

The concentration range of the calibration curve should cover

Table 6
The identification of metabolites of PTX and TTD.

Compound	NO.	Parent and Metabolic Form	Formula	M/z	Error (ppm)	R. T. (min)	Product ions and fragmentation pathway	Biological sample
PTX	M0	Paclitaxel	C47H51NO14Na	876.3213	−0.6	8.37	308.0923, 409.1690, 531.2118, 591.2337, 694.2788, 816.3173	Blood urine microsome
	M1	+OH	C47H51NO15Na	892.3162	0.4	6.58	324.0844(308+OH), 409.1630, 531.1995, 591.2203, 710.2531(694+OH), 832.2960 (816+OH)	Blood urine microsome
	M2	+OH	C47H51NO15Na	892.3162	−0.7	6.87	308.0893, 425.1636(409+OH), 547.1936(531+OH), 607.2136(591+OH),	Microsome
	M3	+OH	C47H51NO15Na	892.3162	−0.3	7.18	308.0896, 409.1632, 547.1957(531+OH), 607.2147(591+OH), 694.2644, 832.2925 (816+OH)	Blood urine microsome
	M4	+2OH	C47H51NO16Na	908.31	−1.3	6.57	160.0068(144+OH), 340.0588(308+2 OH), 607.1918(591+OH), 547.1651(531+OH), 848.2705(816+2 OH)	Blood urine microsome
	M5	+2OH	C47H51NO16Na	908.31	−1.7	6.85	144.0411, 324.0617(308+OH), 607.2155(591+OH), 547.1740(531+OH), 710.2356(609+OH)	Microsome
	M6	+2OH	C47H51NO16Na	908.31	−0.4	7.20	324.0622(308+OH), 563.1672(531+2 OH), 623.1887(591+2 OH), 710.2270(609+OH), 848.2784(816+2OH)	Blood urine microsome
	M7	+2OH	C47H51NO16Na	908.31	0.8	7.58	144.0408, 324.0810(308+OH), 425.1603(409+OH), 485.1782(469+OH), 547.1905 (531+OH), 607.2166(591+OH)	Microsome
	Standard	6-OHPTX	C47H51NO15Na	892.3162	0.3	6.90	308.0893, 425.1636, 547.1936, 607.213,	
TTD	M′0	TTD	C38H42N2O6	623.3116	0.2	19.41	174.0926, 381.1838, 560.2452, 592.2720	Blood urine microsome
	M′1	–CH2-H2+O	C38H42N2O6	623.2752	0.9	10.01	174.0921, 347.1412(365-H20), 365.1514(381-CH4), 379.1674(381-H2), 605.2655(M′0-CH4)	Blood urine microsome
	M′2	–CH2-H2+O	C38H42N2O6	623.2752	1.8	16.7	274.2766(381-CH4), 381.1784, 511.1882(560-NCH5-CH4), 595.2861(M′0-CH4+O-H2O)	Blood urine microsome
	M′3	–CH2	C37H40N2O6	609.2959	3.0	16.34	174.0916, 349.1562(381-CH2-H2O), 367.1665(381-CH2), 382.1893(381+H), 566.2533(580-CH2)	Blood urine microsome
	M′4	–CH2	C37H40N2O6	609.2959	3.3	16.69	192.1025, 381.1828, 546.2291(560-CH2), 578.2560(592-CH2)	Blood urine microsome
	M′5	–CH2	C37H40N2O6	609.2959	3.0	16.87	335.1413(381-CH2-OCH3), 367.1669(381-CH2), 381.1805, 566.2535(609-CH2-OCH3), 578.2532(592-CH2), 592.2695	Blood urine microsome
	M′6	–CH2	C37H40N2O6	609.2959	2.7	17.20	192.1021, 367.1665(381-CH2), 382.1903(381+H), 546.2278(560-CH2), 566.2542(609-CH2-OCH3)	Blood urine microsome
	M′7	–CH2	C37H40N2O6	609.2959	1.6	17.49	176.1076(174+H2), 351.1715(381-CH2-H2O), 367.1666(381-CH2), 566.2553(609-CH2-OCH3), 578.2532(592-CH2)	Urine
	M′8	+OH-CH2	C38H44N2O6	625.3272	1.7	12.88	192.1029, 365.1515(379-CH2), 379.1666(381+OH-CH2), 564.2401(560+H2+OH-CH2), 607.2814(625-H2O)	Blood urine microsome
	M′9	+OH-CH2	C38H44N2O6	625.3272	1.7	13.28	192.1032, 365.1499(379-CH2), 379.1656(381+OH-CH2), 383.1598(381+H2), 564.2407 (560+H2+OH-CH2), 607.2800(625-H2O)	Urine microsome
	M′10	+OH-CH2	C38H44N2O6	625.3272	2.8	14.60	176.0728(174+H2), 379.1687(381+OH-CH2), 383.1613(381+H2), 564.2394 (560+H2+OH-CH2), 607.2822(625-H20)	Urine microsome
	M′11	+OH-CH2	C38H44N2O6	625.3272	2.2	19.47	367.1671(381+OH-CH2), 383.1825(381+H2), 395.2033(381+CH2), 578.2577(592-CH2)	Blood urine microsome
	M′12	–2CH2	C36H38N2O6	595.28026	1.4	13.67	174.0913, 192.1022, 367.1656(381-CH2), 382.1879(381+H), 552.2392(580–2CH2)	Blood urine microsome
	M′13	–2CH2	C36H38N2O6	595.28026	2.3	14.38	178.0881(192-CH2), 353.1511(381–2CH2), 547.2095(595-OCH2-H2O), 564.2390(595-NCH5)	Blood urine microsome
	M′14	–2CH2	C36H38N2O6	595.28026	1.2	14.90	208.0935(206+H2), 335.1394(381–2CH2-H2O), 353.1505(381–2CH2), 367.1672(381-CH2), 552.2416(580–2CH2)	Urine microsome
	M′15	–2CH2	C36H38N2O6	595.28026	0.6	15.30	192.1028, 353.1539(381–2CH2), 367.1646(381-CH2), 458.2075(595-NCH5-C7H8O), 564.2393(595-NCH5)	Urine microsome
	M′16	+O-H2	C38H40N2O7	637.29083	1.3	12.66	144.0822(174-OCH2), 172.0748(192-OCH2), 361.1558(379-H2O), 379.1665(381+OH-H2O), 394.1903(381+OH-H2O-H), 605.2633(637-CH2-H2O)	Blood urine
	M′17	+OH	C38H42N2O7	639.30648	3.6	11.98	174.0931, 353.1491(381–2CH2), 395.2015(381+OH-H2), 566.2521(592+OH-H2O-CH2), 621.2923(639-H2O)	Blood urine microsome
	M′18	+OH	C38H42N2O7	639.30648	4.3	12.20	174.0898, 363.1722(381-H20), 395.1962(381+OH-H2), 592.2699, 623.3027(639-OH)	Blood urine microsome

Table 6 (*continued*)

Compound	NO.	Parent and Metabolic Form	Formula	M/z	Error (ppm)	R. T. (min)	Product ions and fragmentation pathway	Biological sample
	M'19	+OH	C38H42N2O7	639.30648	2.7	12.72	174.0931, 364.1737(381-H2O), 381.1781, 592.2731, 623.2786(639-OH)	Blood urine
								microsome
	M'20	+OH	C38H42N2O7	639.30648	4.2	15.14	174.0912, 379.1666(381+OH-H2O), 394.1884(381+OH-H2O-H), 578.2530(592-CH2), 621.2968(639-H2O)	Blood urine microsome
	M'21	+OH	C38H42N2O7	639.30648	−0.1	15.63	146.0955(174–2CH2), 191.0975(192-H), 379.1687(381+OH-H2O), 397.1720(381+OH), 578.2437(592-CH2), 621.2960(639-H2O)	Blood urine microsome
	M'22	+OH	C38H42N2O7	639.30648	2.9	16.36	174.0878, 365.1526(381-CH4), 397.1747(381+OH), 548.2116(592-OCH2-CH2), 562.2222 (592-OCH2), 621.2970(639-H2O)	Blood urine
	M'23	+OH	C38H42N2O7	639.30648	1.4	16.02	190.0855(192-H2), 397.1756(381+OH), 562.2185(560+H2), 621.2949(639-H20)	Blood urine microsome
	M'24	+OH	C38H42N2O7	639.30648	0.2	19.48	174.0923, 381.1827, 592.2702, 607.2810(639-H2O-CH2), 621.2986(639-H2O)	Urine microsome
	M'25	–3CH2	C35H36N2O6	581.26461	1.2	11.97	194.0812(192+H2), 353.1505(381–3CH2), 550.2234(592–3CH2)	Urine microsome
	M'26	Di-oxidation	C38H42N2O8	655.3009	−0.7	19.47	364.1825(365-H), 381.1819(381+2 OH-H2O-CH2), 395.1973(381+OH-H2), 607.2904(655-H2O-OCH2), 637.2966(655-H20)	Blood urine
	Standard	Fangchinoline	C37H40N2O6	609.2959	2.7	17.20	192.1021, 367.1665, 382.1903, 546.2278, 566.2542, 578.2555	

PTX: paclitaxel. TTD: tetrandrine. 6-OHPTX: 6-hydroxy-paclitaxel. NO.: number. M/z: mass-to-charge ratio. R.T.: retention time.

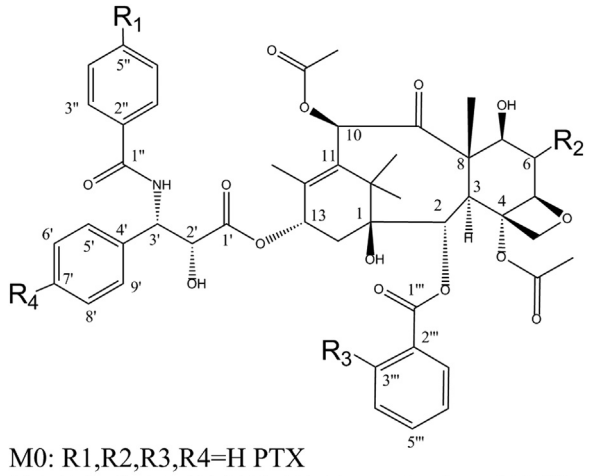

Fig. 7. The metabolites of PTX.

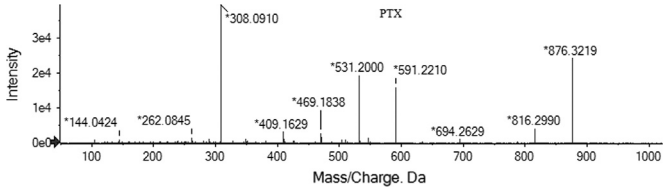

Fig. 8. The MS2 spectrum of PTX.

all the concentrations of samples to be measured. In this method it was 0.25–64 ng/ml. The standard curve built on the ratio between PTX and internal standard and was weighted by $1/x^2$. The obtained correlation coefficients (R^2) was better than 0.99.

3.2.3. *Accuracy, precision,extract recovery*

Intra- and inter-day precision and accuracy are described in Table 2. All results of QC concentrations were within the limits that deviations were up to 15% at three QC concentration levels. This test should be performed during sample analysis, since it is important to control the reproducibility of series samples analysis. In this study, a simple and economic LLE method was applied to satisfy the requirements of pharmacokinetic study. The extract recoveries of three QCs were 86.13%, 96.39%, and 93.18% respectively (Table 1). Therefore, the extract recovery was good enough to meet the requirement of accurate quantity.

3.2.4. *Stability*

The stability of PTX in different conditions were verified and presented in Table 3. All stability data were within a 15% deviation range, suggesting that no significant stability related problems were to be expected during routine analysis and sample store. PTX was stable at room temperature for 24 h, after three freeze–thaw cycle, at −20 °C for two month, and in the auto-sampler 4 °C for 24 h. These results indicate that the freeze–thaw cycle has a greater effect on stability of PTX, so sample should be test as soon as possible and avoid freeze–thaw cycle more than 3 times. The stability of processed sample was acceptable under routine laboratory analysis without incurring any significant loss of detection.

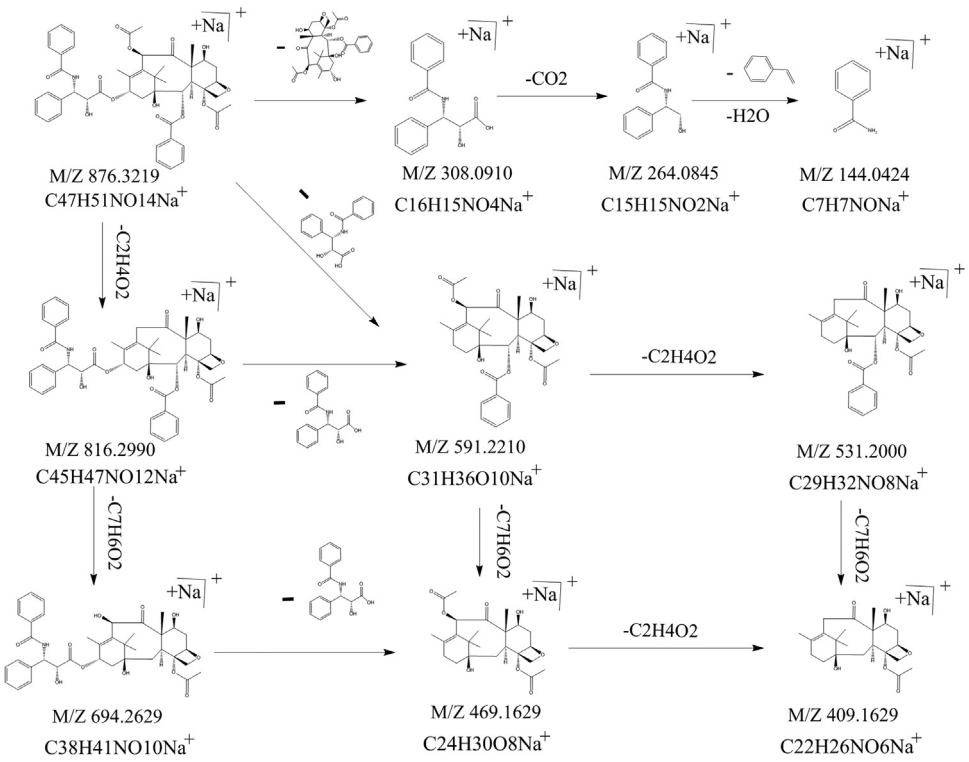

Fig. 9. The fragmentation regularity pattern of PTX.

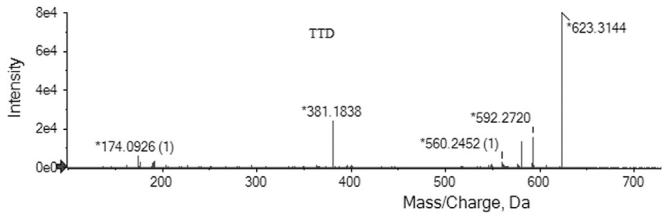

Fig. 10. The MS2 spectrum of TTD.

3.3. Pharmacokinetic study

3.3.1. The effect of TTD on pharmacokinetic of anticancer drug PTX in vitro

To explore the impact of TTD on metabolism of PTX, we performed a liver microsomes experiment. Firstly, we ensured two main metabolites of PTX with good response by incubating the PTX with liver microsome and identified them in Section 3.4. Incubating PTX with different concentrations of TTD in the presence of rats liver microsome, we got the response-time curves of two

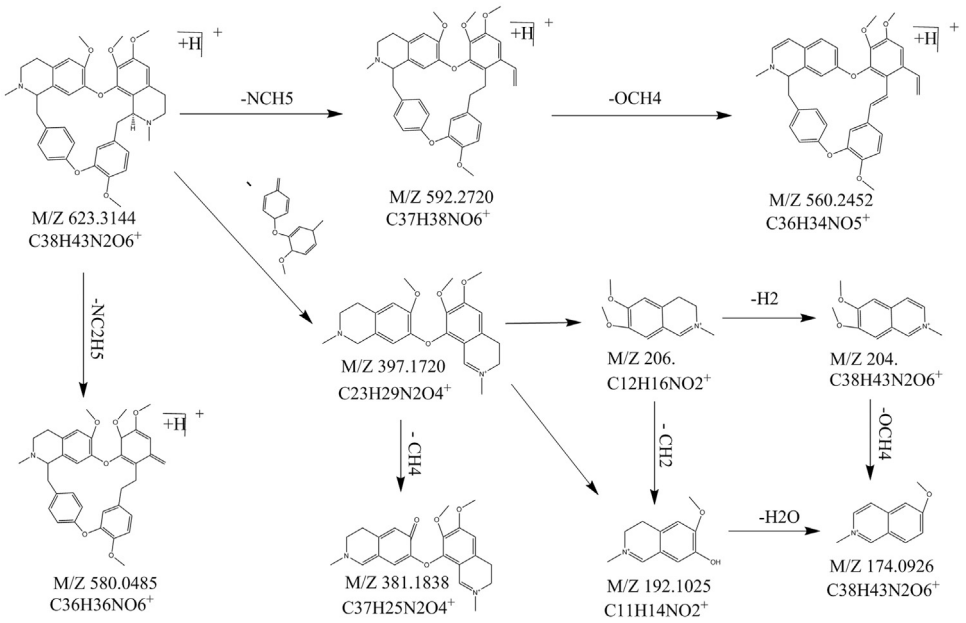

Fig. 11. The fragmentation regularity pattern of TTD.

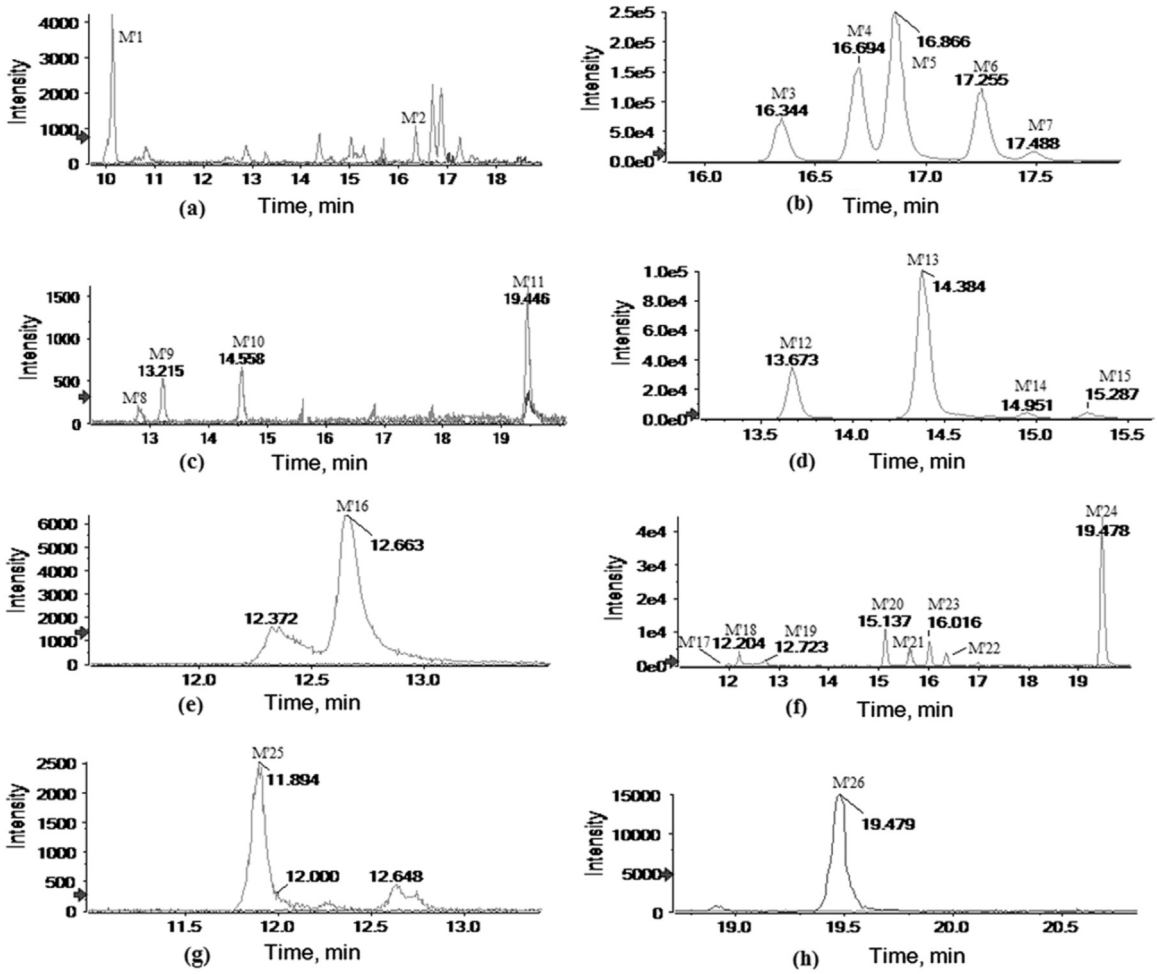

Fig. 12. The spectrum for metabolites of the TTD.

main metabolites of PTX which are illustrated in Figs. 2 and 3. The one is 3′-p-OHPTX at 6.58 min and another is 3′-OHPTX at 7.18 min. Performed statistical analysis of the data, we found significant difference emerged. Compared the drug-combination group with the control group respectively, the p value are 0.0603, 0.0083, 0.0019 for 3′-p-OHPTX. Similarly, the p value are 0.0318, 0.0112, 0.0039 for 3′-OHPTX. Both of the two main metabolites of PTX were dose-dependent inhibited significantly by TTD. This indicated that when PTX combined with TTD, PTX could gain more exposure in vivo because of the inhibition of metabolism by TTD especially when combination with more dose of TTD.

3.3.2. *The effect of TTD on pharmacokinetic of anticancer drug PTX in vivo*

From the results in vitro, we extend to the in-vivo study for exploring TTD effect on metabolism of PTX. PTX combined with different concentration of TTD were injected into the rat's body. The blood samples obtained from series time point were detected, and concentration-time curves are illustrated in Fig. 4 and the pharmacokinetics parameters are summarized in Table 4. As is shown, we can see the distribution half-life ($t_{1/2}\alpha$) and elimination half-life ($t_{1/2}\beta$) were extended with the increase concentration of TTD, as well as AUC. The response-time curves of 3′-OHPTX are shown in Fig. 5. Compared the drug-combination group with the control group respectively, the p value are 0.1410, 0.0096 for metabolite of PTX. With the increased concentration of TTD, the metabolite of PTX was inhibited significantly. What's more, compared with the response-time curve of PTX metabolites in vitro, we can see the results about 3′-OHPTX was consistent. In other words, the TTD could inhibit the metabolite of PTX to increase the exposure of PTX no matter in vivo and in vitro. Therefore, TTD not only had a synergistic effect on improving the antitumor efficacy of PTX [22,29] but also could change the pharmacokinetic behavior of PTX in our study.

The half-life of PTX administered alone is similar to previous report about Pharmacokinetic Study of PTX [50]. In our study, while PTX combined with the middle concentration of TTD, its pharmacokinetic parameters emerged significant difference ($p=0.0491$). However, compared the high drug combination group with control group, there is no significant difference ($p=0.2678$) for PTX. This may due to the statistic deviation resulted from little original date ($n=5$). In this part, although we also found 3′-p-OHPTX in 30 μl prepared plasma samples, its response is lower than 3′-OHPTX and it was difficult to be detected at all-time points. So that, there is no response-time curves of 3′-p-OHPTX.

3.4. *The affinity study*

As a broad-spectrum anti-cancer drug, PTX could prevent cell division cycle by targeting microtubulin [1]. There are some metabolic differences between different species. Although 3′-p-OHPTX and 3′-OHPTX are the main metabolites of PTX in rat. For human being, the 6-OHPTX is the main metabolite of PTX as well as 3′-p-OHPTX [55]. In this study, we determined the affinity between microtubulin and PTX, as well as 6-OHPTX, TTD, mixture of them respectively (Table 5). From the affinity constant KD value

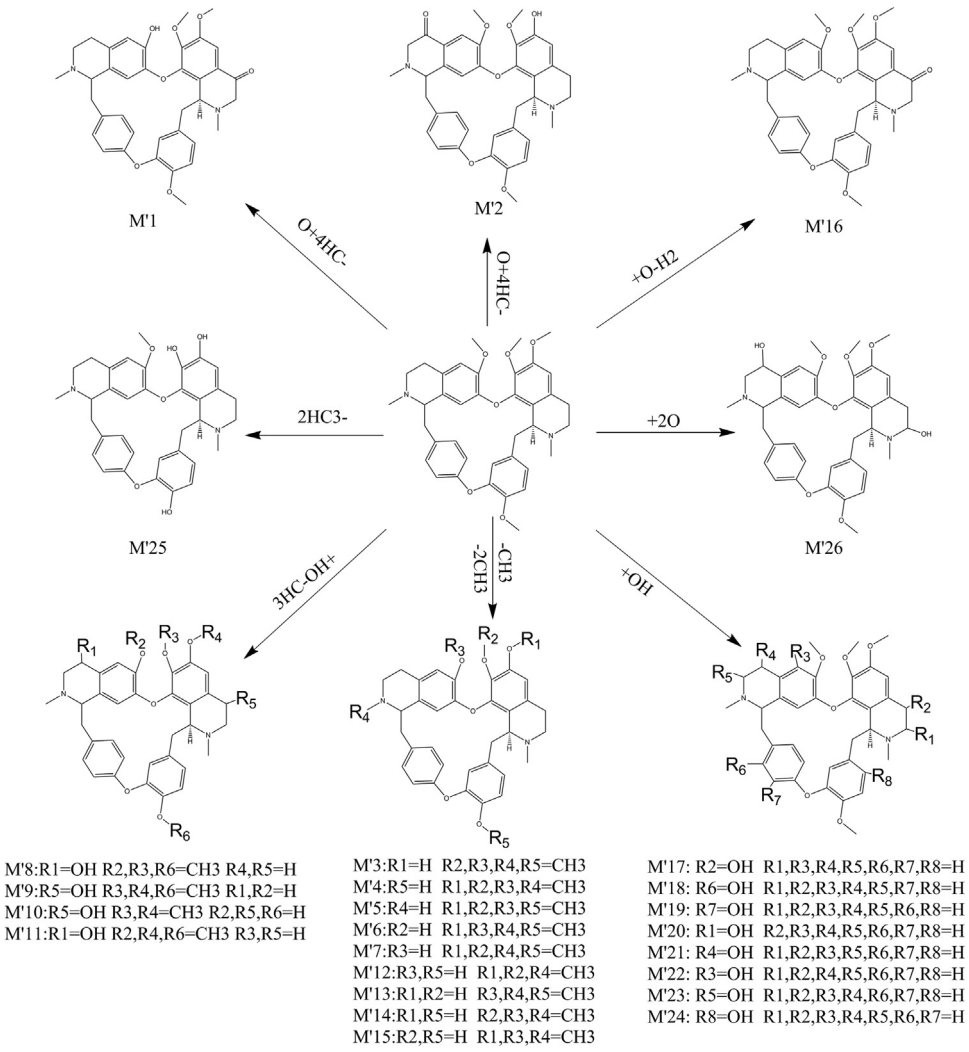

Fig. 13. The fragmentation regularity pattern of TTD.

difference, TTD could not affect the affinity between PTX and microtubulin (1.71E-06 vs. 1.23E-06 vs. 1.05E-04). The affinity between PTX and microtubulin was similar to the affinity between 6-OHPTX and microtubulin (1.71E-06 vs. 1.05E-06). The mixture of PTX and 6-OHPTX (1:1) shown the same affinity to microtubuline. The affinity can be seen as an indicator for efficacy evaluation. Therefore, although TTD affect the metabolism of PTX, the whole efficacy of PTX may not be affected and TTD could not affect PTX binding to microtubulin. For this result, we have a hypothesis that TTD has an influence on the metabolite of PTX, but TTD and the main metabolites of PTX probably don't affect PTX's biological targeting, so the effect of its pharmacological action needs to be further confirmed.

3.5. Identification of metabolites

3.5.1. The metabolites of PTX

We totally identified 7 metabolites of PTX in blood, urine and incubation of microsome samples. Among of them, M1, M3, M4, M6 could be found in all these biological samples. M2, M5, M7 just were found in incubation of microsome (Fig. 6). All of these metabolites are mono- or di-hydroxylation based on the structure of parent and the detail metabolites information is shown in the following Table 6. And the formulations are described in the Fig. 7. The main MS^2 fragments of parent are 144.0424, 308.0910, 409.1629, 459.1838, 531.2000, 591.2210, 876.3219 etc. (Fig. 8). According to the standard of 6-OHPTX, we found the M2 was 6-OHPTX for the same MS^2 spectrum and retention time (Table 6). The other hydroxyl replaced position was speculated by retention time and fragmentation differences between parent compound and its metabolites and the fragmentation regularity pattern of PTX is shown in Fig. 9.

3.5.2. The metabolites of TTD

Considering identification the TTD and its metabolites, we changed the chromatographic condition. There was a problem when we used the same LC–MS condition to analyse the metabolites of TTD. Because the low abundance metabolites of TTD were disturbed by strong peak tails of TTD in the same LC condition. To solve the problem, 0.1% ammonia were added to the mobile phase A. What's more, the gradient elution changed as follow: 0–10 min,10–40%B; 10–23 min,40–80%B; 23–25 min,80–95%B; 25.1–30 min,10%B. Totally 26 metabolites of TTD were identified in blood, urine and incubation samples (Fig. 12). The response of metabolites was different in different biological sample. All metabolites were found in urine sample, 23 metabolites were found in incubation sample and 19 metabolites in blood sample. TTD were extensively metabolized no matter in vitro and in vivo. The metabolites of TTD are shown in the Table 6. The possible metabolic forms are illuminated in Fig. 13. The main MS^2 fragments of parent are 174.0926, 381.1838, 560.2452, 592.2720, 623,3144 etc. (Fig. 10). According to the standard of fangchinoline,

we found the M′6 was fangchinoline for similarly MS^2 spectrum and retention time (Table 6). The other replaced position was speculated by retention time and fragmentation differences between parent compound and its metabolites and the fragmentation regularity pattern of TTD is shown in Fig. 11. However, for various potential replaceable positions, some structural formulas were not confirmed completely just according to the MS information. So the further identification should depend on other means such as NMR (nuclear magnetic resonance), IR (infrared radiation spectroscopy) and so on. TTD was metabolized extensively both in vitro and in vivo, but demethylation and hydroxylation are the primary metabolic form in the process of phase one metabolism. As a botanical drug, TTD is a potential reversal agents for multi-drug resistance with high security, there were few reports for study the identification about the metabolites of TTD in previous studies [56]. Our identification result may be able to support reference for further study for TTD.

4. Conclusions

The verified method based on IDA acquisition is sensitive accurate and effective for applying to the simultaneous determination of PTX and identification metabolites in blood, urine and live microsome incubation samples. In this established method, the LLOQ could reach 0.25 ng/ml after sample preparation just used 30 μl plasma, so that it was sensitive enough to determinate the PTX. And no significant interference was caused by endogenous compounds. We used this method successfully to evaluation the drug–drug interaction between PTX and TTD in vitro and in vivo. The results indicated that TTD could dose-dependent inhibit the metabolism of PTX and increase the drug exposure of PTX no matter in vitro and in vivo. What's more, we identified 7 metabolites of PTX and 26 metabolites of TTD systematically and comprehensively in blood, urine and live microsome incubation samples. Hydroxylation of PTX is its main metabolic form and TTD could be extensively metabolized in vitro and in vivo. 3′-OHPTX as another main metabolites of PTX was found except 3′-p-OHPTX in rat. We also preliminary evaluated the affinity between PTX and microtubulin, the affinity between metabolite of PTX and microtubulin, and the affinity between TTD and microtubulin. The results shown TTD and the main metabolites of PTX probably don't affect PTX's biological targeting and the effect of its pharmacological action needs to be further studied.

Acknowledgments

This work was supported by Screening Platform Construction Projects of School of Pharmacy, Fudan University. We also thank Professor Qing Mu and Dr. Jiekai Cheng for their valuable suggestions.

References

[1] C. Hansch, R.P. Verma, Understanding tubulin/microtubule-taxane interactions: a quantitative structure – activity relationship study, Mol. Pharm. 5 (2008) 151–161.
[2] C.M. Spencer, D. Faulds, Paclitaxel – a review of its pharmacodynamic and pharmacokinetic properties and therapeutic potential in the treatment of cancer, Drugs 48 (1994) 794–847.
[3] Yu Yu, S. Gaillard, J.M. Phillip, Inhibition of spleen tyrosine kinase potentiates paclitaxel-induced cytotoxicity in ovarian cancer cells by stabilizing microtubules, Cancer Cell 28 (2015) 82–96.
[4] G. Dranitsaris, B. Yu, L. Wang, W. Sun, Y. Zhou, J. King, S. Kaura, A. Zhang, P. Yuan, Abraxane(R) versus Taxol(R) for patients with advanced breast cancer: a prospective time and motion analysis from a Chinese health care perspective, J. Oncol. Pharm. Pract. 22 (2016) 205–211.
[5] L.C. Villaruz, M.A. Socinski, Is there a role of nab-paclitaxel in the treatment of advanced non-small cell lung cancer? The data suggest yes, Eur. J. Cancer 56 (2016) 162–171.
[6] C. Wang, L.B. Guo, J.Y. Ma, Y.M. Li, H.M. Liu, Establishment and characterization of a paclitaxelresistant human esophageal carcinoma cell line, Int. J. Oncol. 43 (2013) 1607–1617.
[7] F. Wang, D. Zhang, Q. Zhang, Y. Chen, D. Zheng, L. Hao, C. Duan, L. Jia, G. Liu, Y. Liu, Synergistic effect of folate-mediated targeting and verapamil-mediated P-gp inhibition with paclitaxel-polymer micelles to overcome multi-drug resistance, Biomaterials 32 (2011) 9444–9456.
[8] B. Guo, D.J. Villeneuve, S.L. Hembruff, A.F. Kirwan, D.E. Blais, M. Bonin, A. M. Parissenti, Cross-resistance studies of isogenic drug-resistant breast tumor cell lines support recent clinical evidence suggesting that sensitivity to paclitaxel may be strongly compromised by prior doxorubicin exposure, Breast Cancer Res. Treat. 85 (2004) 31–51.
[9] J.N. Orina, A.M. Calcagno, C.P. Wu, S. Varma, J. Shih, M. Lin, G. Eichler, J. N. Weinstein, Y. Pommier, S.V. Ambudkar, M.M. Gottesman, J.P. Gillet, Evaluation of current methods used to analyze the expression profiles of ATP-binding cassette transporters yields an improved drug-discovery database, Mol. Cancer Ther. 8 (2009) 2057–2066.
[10] E. Bernabeu, L. Gonzalez, M. Cagel, E.P. Gergic, M.A. Moretton, D.A. Chiappetta, Novel Soluplus®—TPGS mixed micelles for encapsulation of paclitaxel with enhanced in vitro cytotoxicity on breast and ovarian cancer cell lines, Colloid Surf. B. 140 (2016) 403–411.
[11] J. van Asperen, O. van Tellingen, A. Sparreboom, A.H. Schinkel, P. Borst, W. J. Nooijen, J.H. Beijnen, Enhanced oral bioavailability of paclitaxel in mice treated with the P-glycoprotein blocker SDZ PSC 833, Br. J. Cancer 76 (1997) 1181–1183.
[12] W. Xu, J.J. Beitler, H. Wang, M.J. Lee, Honokiol enhances paclitaxel efficacy in multi-drug resistant human cancer model through the induction of apoptosis, PLoS One 9 (2014) e86369.
[13] C.D. Britten, S.D. Baker, L.J. Denis, T. Johnson, R. Drengler, L.L. Siu, Oral paclitaxel and concurrent cyclosporin a: targeting clinically relevant systemic exposure to paclitaxel, Clin. Cancer Res. 6 (2000) 3459–3468.
[14] J.R. Diamond, B. Wu, N. Agarwal, D.W. Bowles, E.T. Lam, T.L. Werner, E. Rasmussen, E. Gamelin, F. Soto, G. Friberg, Y. Sun, S. Sharma, Pharmacokinetic drug-drug interaction study of the angiopoietin-1/angiopoietin-2-inhibiting peptibody trebananib (AMG 386) and paclitaxel in patients with advanced solid tumors, Invest. New Drug 33 (2015) 691–699.
[15] T.E. Kim, H. Lee, K.S. Lim, S.H. Lee, S.H. Yoon, K.M. Park, H. Han, S.G. Shin, I. J. Jang, K.S. Yu, J.Y. Cho, Effects of HM30181, a P-glycoprotein inhibitor, on the pharmacokinetics and pharmacodynamics of loperamide in healthy volunteers, Br. J. Clin. Pharm. 78 (2014) 556–564.
[16] M. Tsai, Z. Lu, M.G. Wientjes, J.L.S. Au, Paclitaxel-loaded polymeric microparticles: quantitative relationships between in vitro drug release rate and in vivo pharmacodynamics, J. Control. Release 172 (2013) 737–744.
[17] Y.J. Ye, Y. Wang, K.Y. Lou, Y.Z. Chen, R.J. Chen, F. Gao, The preparation, characterization, and pharmacokinetic studies of chitosan nanoparticles loaded with paclitaxel/dimethyl-beta-cyclodextrin inclusion complexes, Int. J. Nanomed. 10 (2015) 4309–4319.
[18] J. Mo, P.K. Eggers, C.L. Raston, L.Y. Lim, Development and validation of a LC/TOF MS method for the determination of carboplatin and paclitaxel in nanovesicles, Anal. Bioanal. Chem. 406 (2014) 2659–2667.
[19] L.W. Fu, Y.M. Zhang, Y.J. Liang, X.P. Yang, Q.C. Pan, The multidrug resistance of tumour cells was reversed by tetrandrine in vitro and in xenografts derived from human breast adenocarcinoma MCF-7/adr cells, Eur. J. Cancer 38 (2002) 418–426.
[20] L. Fu, Y. Liang, L. Deng, Y. Ding, L. Chen, Y. Ye, X. Yang, Q. Pan, Characterization of tetrandrine, a potent inhibitor of P-glycoprotein-mediated multidrug resistance, Cancer Chemother. Pharm. 53 (2004) 349–356.
[21] Y.F. Sun, M. Wink, Tetrandrine and fangchinoline, bisbenzylisoquinoline alkaloids from Stephania tetrandra can reverse multidrug resistance by inhibiting P-glycoprotein activity in multidrug resistant human cancer cells, Phytomedicine 21 (2014) 1110–1119.
[22] Z. Zhang, J. Yan, K. Xu, Z. Ji, L. Li, Tetrandrine reverses drug resistance in isoniazid and ethambutol dual drug-resistant Mycobacterium tuberculosis clinical isolates, BMC Infect. Dis. 15 (2015).
[23] W.L. Xu, H.L. Shen, Z.F. Ao, B.A. Chen, W. Xia, F. Gao, Y.N. Zhang, Combination of tetrandrine as a potential-reversing agent with daunorubicin, etoposide and cytarabine for the treatment of refractory and relapsed acute myelogenous leukemia, Leuk. Res. 30 (2006) 407–413.
[24] P.L. Kuo, C.C. Lin, Tetrandrine-induced cell cycle arrest and apoptosis in Hep G2 cells, Life Sci. 73 (2003) 243–252.
[25] B.C. Jang, K.J. Lim, J.H. Paik, J.W. Cho, W.K. Baek, M.H. Suh, J.B. Park, T.K. Kwon, Tetrandrine-induced apoptosis is mediated by activation of caspases and PKC-δ in U937 cells, Biochem. Pharmacol. 67 (2004) 1819–1829.
[26] Y. Hou, T. Guo, C. Wu, X. He, Effect of Tetrandrine Combined with Epirubicin on the Growth of Human Breast Carcinoma Multidrug Resistance Cell Line, Yakugaku Zasshi 128 (2008) 663–666.
[27] J. Wei, B. Liu, L. Wang, X. Qian, Y. Ding, L. Yu, Synergistic interaction between tetrandrine and chemotherapeutic agents and influence of tetrandrine on chemotherapeutic agent-associated genes in human gastric cancer cell lines, Cancer Chemother. Pharm. 60 (2007) 703–711.
[28] H.S. Cho, S.H. Chang, Y.S. Chung, J.Y. Shin, S.J. Park, E.S. Lee, S.K. Hwang, J. T. Kwon, A.M. Tehrani, M. Woo, M.S. Noh, H. Hanifah, H. Jin, C.X. Xu, M.H. Cho,

Synergistic effect of ERK inhibition on tetrandrine-induced apoptosis in A549 human lung carcinoma cells, J. Vet. Sci. 10 (2009) 23–28.
[29] X.M. Zhu, M.H. Sui, W.M. Fan, In vitro and in vivo characterizations of tetrandrine on the reversal of P-glycoprotein-mediated drug resistance to paclitaxel, Anticancer Res. 25 (2005) 1953–1962.
[30] J.R. Diamond, B. Wu, N. Agarwal, D.W. Bowles, E.T. Lam, T.L. Werner, E. Rasmussen, E. Gamelin, F. Soto, G. Friberg, Y. Sun, S. Sharma, Pharmacokinetic drug-drug interaction study of the angiopoietin-1/angiopoietin-2-inhibiting peptibody trebananib (AMG 386) and paclitaxel in patients with advanced solid tumors, Invest. New Drugs 33 (2015) 691–699.
[31] H. Nokihara, N. Yamamoto, Y. Ohe, M. Hiraoka, T. Tamura, Pharmacokinetics of weekly paclitaxel and feasibility of dexamethasone taper in japanese patients with advanced non–small cell lung cancer, Clin. Ther. 38 (2016) 338–347.
[32] M. Hou, C. Lu, T. Tsai, Effects of Jia-Wei-Xiao-Yao-San on the peripheral and lymphatic pharmacokinetics of paclitaxel in rats, Evid.-Based Complement. Altern. (2016) 1–10.
[33] R.J. Kathawala, L. Wei, N. Anreddy, The small molecule tyrosine kinase inhibitor NVP-BHG712 antagonizes ABCC10-mediated paclitaxel resistance: a preclinical and pharmacokinetic study, Oncotarget 6 (2014) 510–521.
[34] J. Zhang, B. Yu, X.Q. Zhang, Z.F. Sheng, S.J. Li, Z.J. Wang, X.Y. Cui, S.Y. Cui, Y. H. Zhang, Tetrandrine, an antihypertensive alkaloid, improves the sleep state of spontaneously hypertensive rats (SHRs), J. Ethnopharmacol. 151 (2014) 729–732.
[35] C.Y. Kwan, F.I. Achike, Tetrandrine and related bis-benzylisoquinoline alkaloids from medicinal herbs: cardiovascular effects and mechanisms of action, Acta Pharmacol. Sin. 23 (2002) 1057–1068.
[36] G. Teng, D. Svystonyuk, H.E.M. Mewhort, J.D. Turnbull, D.D. Belke, H.J. Duff, P. W.M. Fedak, Tetrandrine reverses human cardiac myofibroblast activation and myocardial fibrosis, Am. J. Physiol. Heart C 308 (2015) H1564–H1574.
[37] Y.Q. Shan, Y.P. Zhu, J. Pang, Tetrandrine potentiates the hypoglycemic efficacy of berberine by inhibiting P-glycoprotein function, Biol. Pharm. Bull. 36 (2013) 1562–1569.
[38] T. Kudo, Y. Ozaki, T. Kusano, E. Hotta, Y. Oya, S. Komatsu, H. Goda, K. Ito, Effect of buffer conditions on CYP2C8-mediated paclitaxel 6alpha-hydroxylation and CYP3A4-mediated triazolam alpha- and 4-hydroxylation by human liver microsomes, Xenobiotica 46 (2016) 241–246.
[39] C.M. Lin, Y.Q. Jiang, A.G. Chaudhary, J.M. Rimoldi, D.G.I. Kingston, E. Hamel, A convenient tubulin-based quantitative assay for paclitaxel (Taxol) derivatives more effective in inducing assembly than the parent compound, Cancer Chemother. Pharm. 38 (1996) 136–140.
[40] S.I. Suye, S. Tandel, A. Mulchandani, A receptor protein-based bioassay for quantitative determination of paclitaxel, Anal. Chem. 69 (1997) 3633–3635.
[41] D. Fraier, V. Cenacchi, E. Frigerio, Determination of a new polymer-bound paclitaxel derivative (PNU 166945), free paclitaxel and 7-epipaclitaxel in dog plasma and urine by reversed-phase high-performance liquid chromatography with UV detection, J. Chromatogr. A 797 (1998) 295–303.
[42] C. Bicamumpaka, M. Page, Development of a fluorescence polarization immunoassay (for the quantitative determination of paclitaxel, J. Immunol. Methods 212 (1998) 1–7.
[43] T.M. Holgado, M.C. Quintana, J.M. Pinilla, Electrochemical study of taxol (paclitaxel) by cathodic stripping voltammetry: determination in human urine, Microchem. J. 74 (2003) 99–104.
[44] S.H. Sheikh, B.A. Abela, A. Mulchandani, Development of a fluorescence immunoassay for measurement of paclitaxel in human plasma, Anal. Biochem. 283 (2000) 33–38.
[45] P. Guo, J.G. Ma, S.L. Li, J.M. Gallo, Determination of paclitaxel in mouse plasma and brain tissue by liquid chromatography–mass spectrometry, J. Chromatogr. B 798 (2003) 79–86.
[46] H. Green, K. Vretenbrant, B. Norlander, C. Peterson, Measurement of paclitaxel and its metabolites in human plasma using liquid chromatography/ion trap mass spectrometry with a sonic spray ionization interface, Rapid Commun. Mass Spectrom. 20 (2006) 2183–2189.
[47] X.Y. Tong, J.P. Zhou, Y. Tan, Determination of paclitaxel in rat plasma by LC-MS-MS, J. Chromatogr. Sci. 44 (2006) 266–271.
[48] M.A. Fernández-Peralbo, F. Priego-Capote, M.D. Luque De Castro, A. Casado-Adam, A. Arjona-Sánchez, F.C. Muñoz-Casares, LC–MS/MS quantitative analysis of paclitaxel and its major metabolites in serum, plasma and tissue from women with ovarian cancer after intraperitoneal chemotherapy, J. Pharm. Biomed. 91 (2014) 131–137.
[49] X.Y. Tong, J.P. Zhou, Y. Tan, Liquid chromatography/tandem triple-quadrupole mass spectrometry for determination of paclitaxel in rat tissues, Rapid Commun. Mass Spectrom. 20 (2006) 1905–1912.
[50] H. Lian, J. Sun, T. Zhang, A rapid and sensitive determination of paclitaxel in rat plasma by UPLC-MS/MS method: application to a pharmacokinetic study, Asian J. Pharm. Sci. 8 (2013) 199–205.
[51] H. Yamaguchi, A. Fujikawa, H. Ito, et al., A rapid and sensitive LC/ESI–MS/MS method for quantitative analysis of docetaxel in human plasma and its application to a pharmacokinetic study, J. Chromatogr. B 893–894 (2012) 157–161.
[52] J.J.M.A. Hendrikx, M.J.X. Hillebrand, et al., A sensitive combined assay for the quantification of paclitaxel, docetaxel and ritonavir in human plasma using liquid chromatography coupled with tandem mass spectrometry, J. Chromatogr. B 879 (2011) 2984–2990.
[53] G.A. Papalia, M. Baer, K. Luehrsen, H. Nordin, P. Flynn, D.G. Myszka, High-resolution characterization of antibody fragment/antigen interactions using Biacore T100, Anal. Biochem. 359 (2006) 112–119.
[54] R.J. Hosse, L. Tay, M.K. Hattarki, L. Pontes-Braz, L.A. Pearce, S.D. Nuttall, O. Dolezal, Kinetic screening of antibody–Im7 conjugates by capture on a colicin E7 DNase domain using optical biosensors, Anal. Biochem. 385 (2009) 346–357.
[55] Y. Wang, M. Wang, H. Qi, P. Pan, T. Hou, J. Li, G. He, H. Zhang, Pathway-dependent inhibition of paclitaxel hydroxylation by kinase inhibitors and assessment of drug-drug interaction potentials, Drug Metab. Dispos. 42 (2014) 782–795.
[56] X. Wang, X. Liu, X. Xu, T. Zhu, F. Shi, K. Qin, B. Cai, Screening and identification of multiple constituents and their metabolites of Fangji Huangqi Tang in rats by ultra-high performance liquid chromatography coupled with quadrupole time-of-flight tandem mass spectrometry basing on coupling data processing techniques, J. Chromatogr. B 985 (2015) 14–28.